Investigation of the effects of the transition from an ideal- to an extended-MHD model on peeling-ballooning modes

J R King[1], S E Kruger[1], P B Snyder[2]

[1]Tech-X Corporation
[2]General Atomics

CEMM meeting
Sherwood Fusion Theory Conference 2013

Previous work with the NIMROD code studying tokamak edge modes with a relatively high q_{95} (6-7) encountered difficulties.

- The poloidal-resolution weak scaling for these cases was limited by the amount of system memory (RAM) available.
- NIMROD cases with an ideal-like MHD model at this limited resolution did not agree ELITE computations.
- This motivated memory profiling of the NIMROD code, which identified a key memory-scaling bottleneck that has now been overcome.
- The elimination of this memory-scaling bottleneck has enabled a successful benchmark between ELITE and NIMROD on the 'Meudas' case, which was previously used as the basis of a benchmark between ELITE and M3D-C1 [1].
- In addition, we are now able to converge on cases that make use of NIMROD's extended-MHD model, which includes the use of anisotropic thermal conduction, ion gyroviscosity, and two-fluid and drift effects through the use of a generalized Ohm's law.

[1] Ferraro et al. Phys. Plasmas 102508 (2010)

We have a new routine (dsta) that improves the memory efficiency during the export of NIMROD's sparse matrix to external solvers.

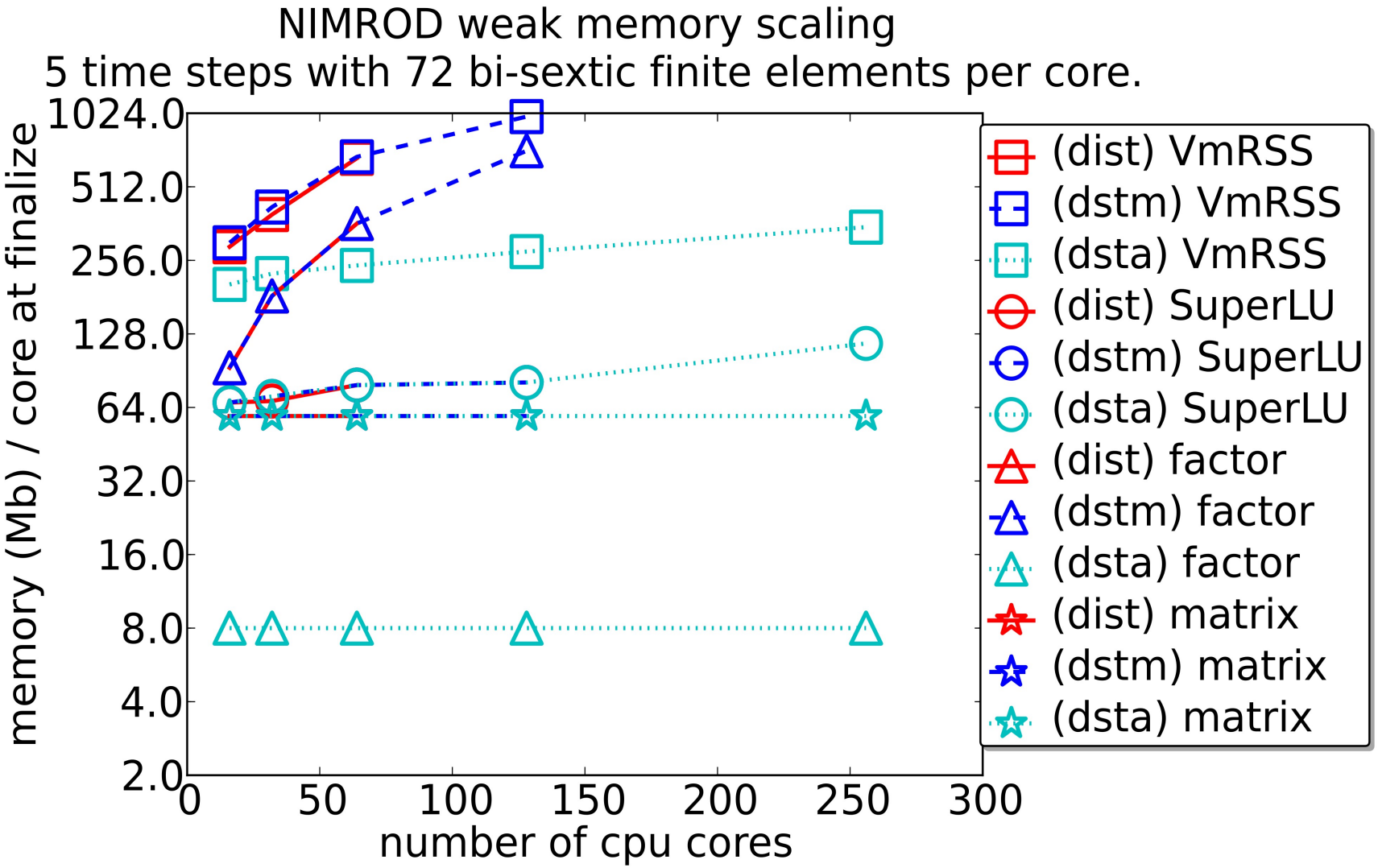

The new distributed sparsity pattern interface (dsta) is at least as fast as the previous implementations.

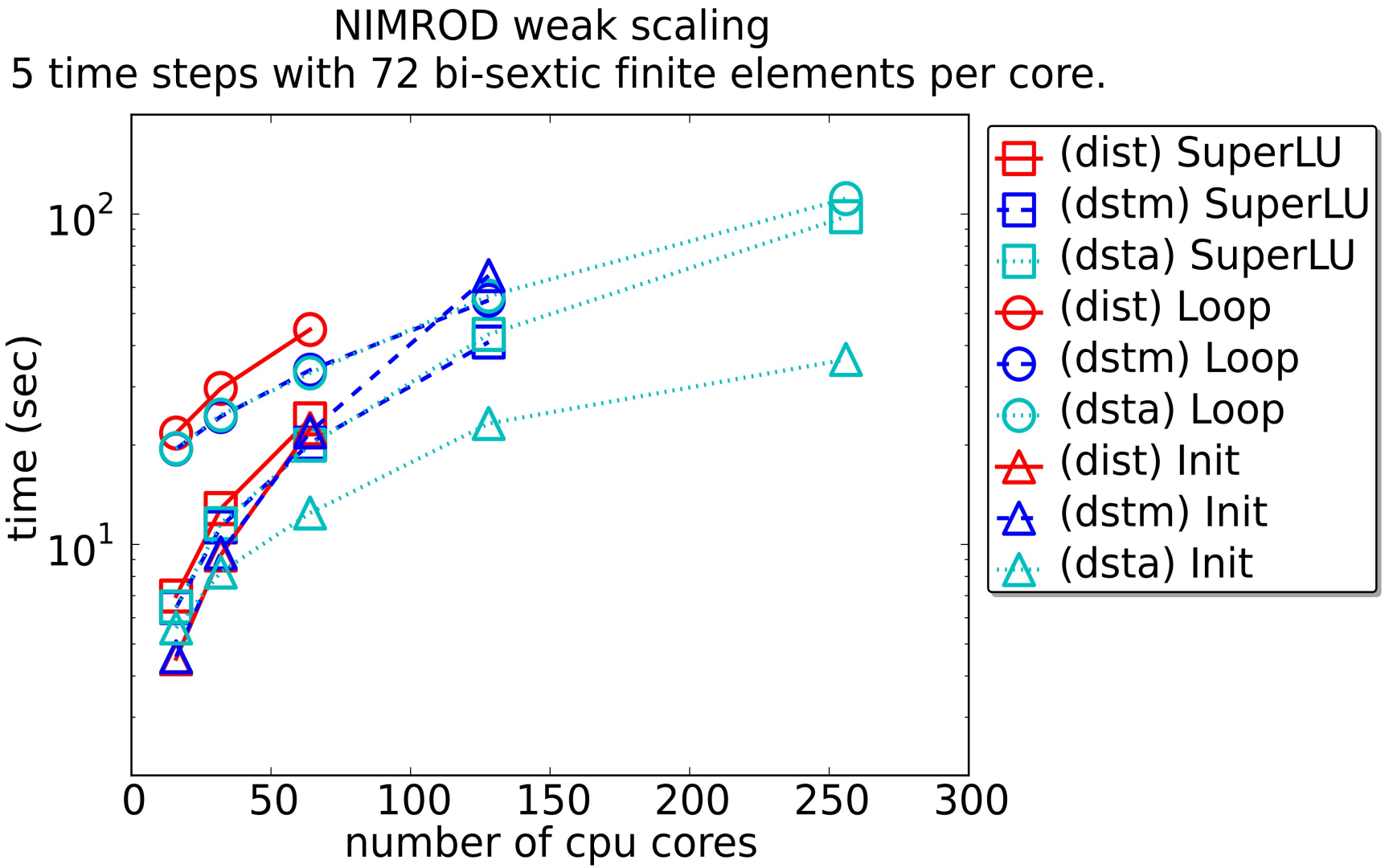

This example case uses SuperLU to obtain the LU factor decomposition and solves for only five time steps. Typical linear-physics cases require thousands of time steps without matrix factorization, thus the time-to-solution scaling shown here is for comparison only and not characteristic of a typical use case.

This new capability enables new simulations that were previously unachievable.

- The maximum achievable amount of poloidal-mesh resolution has been increased.
- As the plots on the previous slides implicitly indicate, the old routines (dist and dstm) were not able to scale to the same resolution as the new routine (dsta).
- With the new routine (dsta), optimizations are made to the construction and handling of the matrix sparsity pattern and the loading of the distributed matrix values that belong to other processors.
- This allows spatial convergence for cases that previously encountered a memory-scaling limitation.

With a relatively-large edge safety factor (q_{95}~6-7), edge simulations require large poloidal resolution.

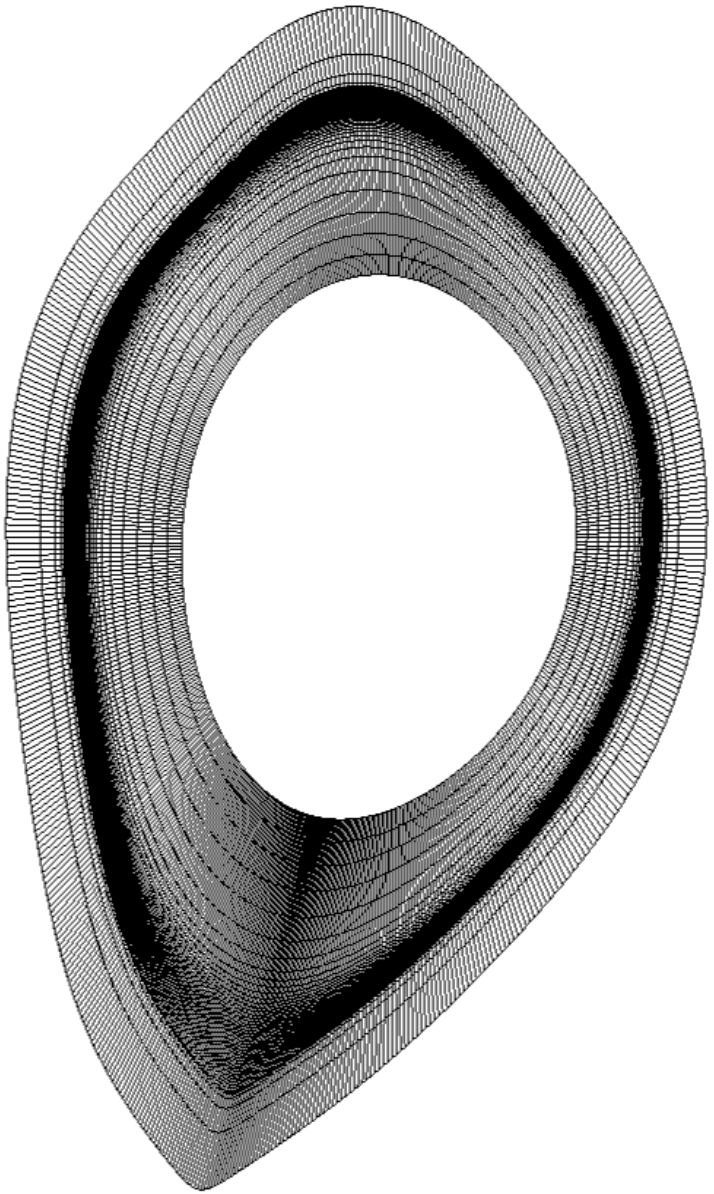

48x512 FE mesh

- Computations are performed with the NIMROD code on Titan, where a single mode computation uses 128-512 cores for less than an hour.
- Computations use a packed, flux-aligned, annular, 48x512 finite-element mesh with bi-quartic to bi-septic spectral elements.
- This resolution could be increased even further.
- For comparison, the previous memory-limited cases used a 32x288 finite-element mesh.

We are now able to benchmark NIMROD with ELITE results on a reconstruction with a diverted-plasma and a relatively-high q_{95}.

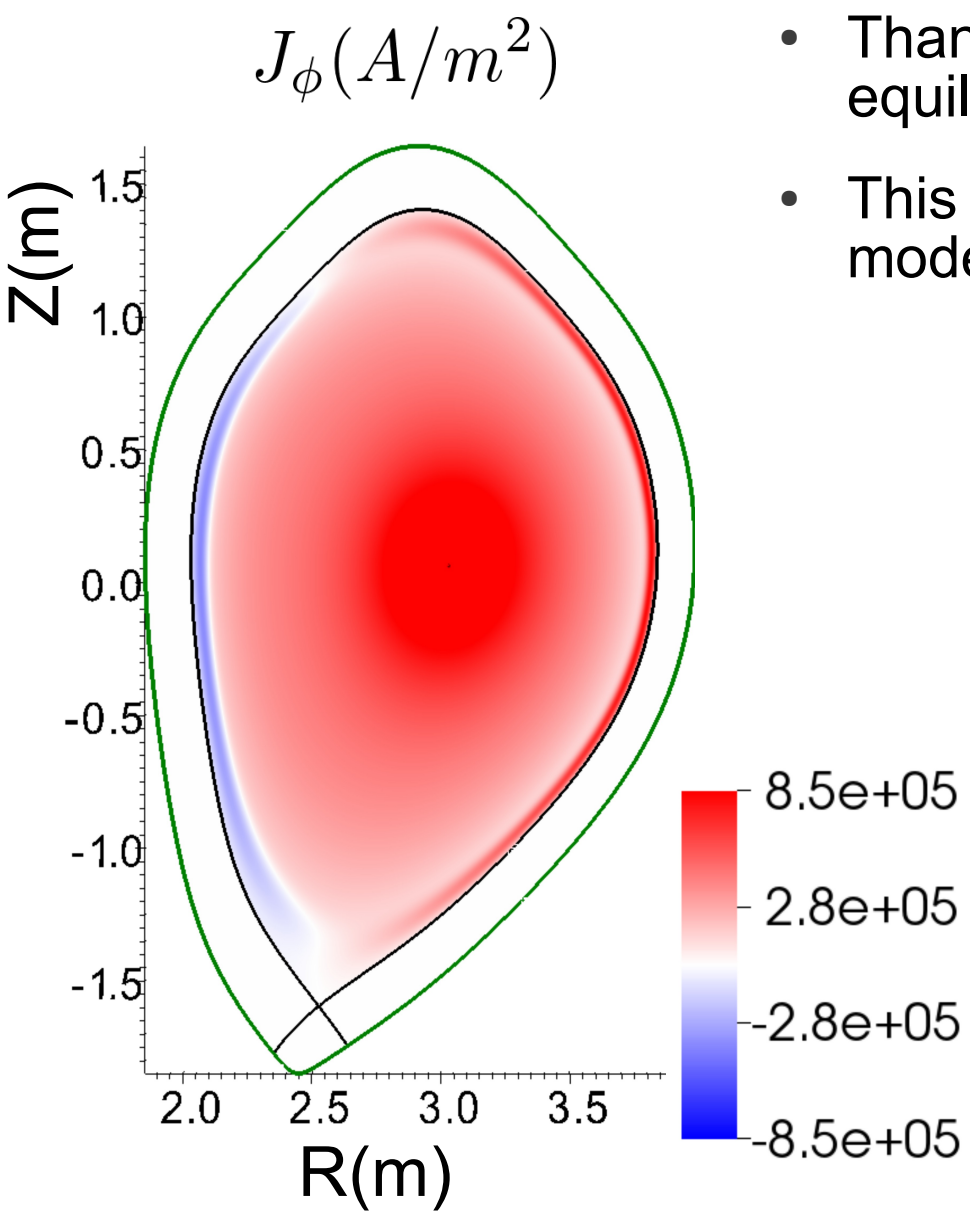

- Thanks to N. Aiba for providing this benchmark equilibria.
- This equilibria is a reconstruction of diverted H-mode plasma in JT-60U.

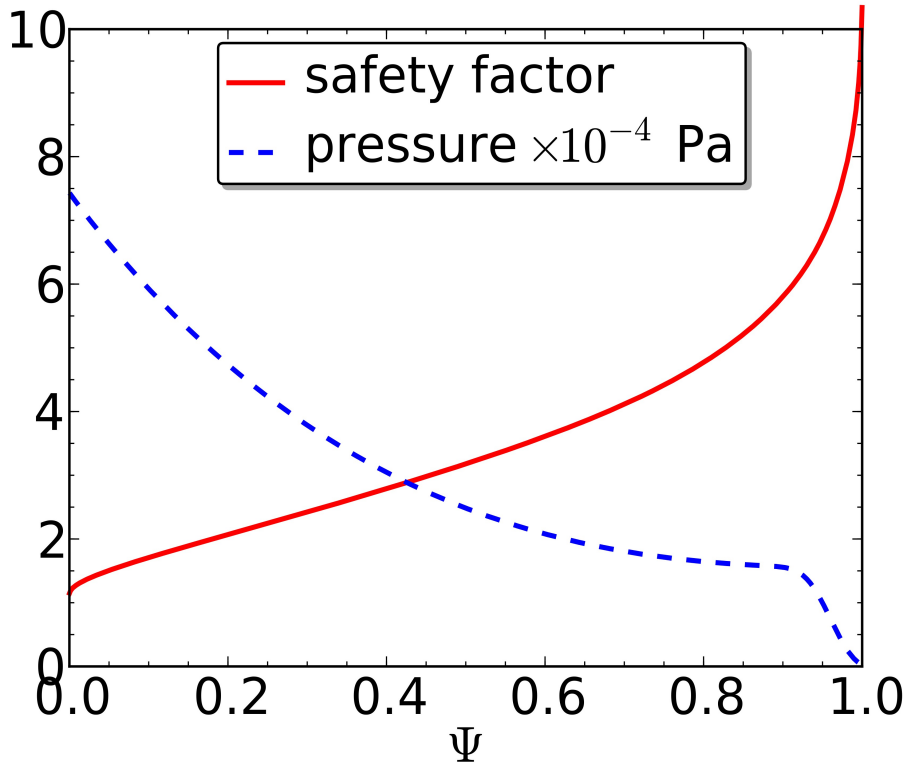

The ideal-like spectrum computed by NIMROD is comparable to that computed by ELITE.

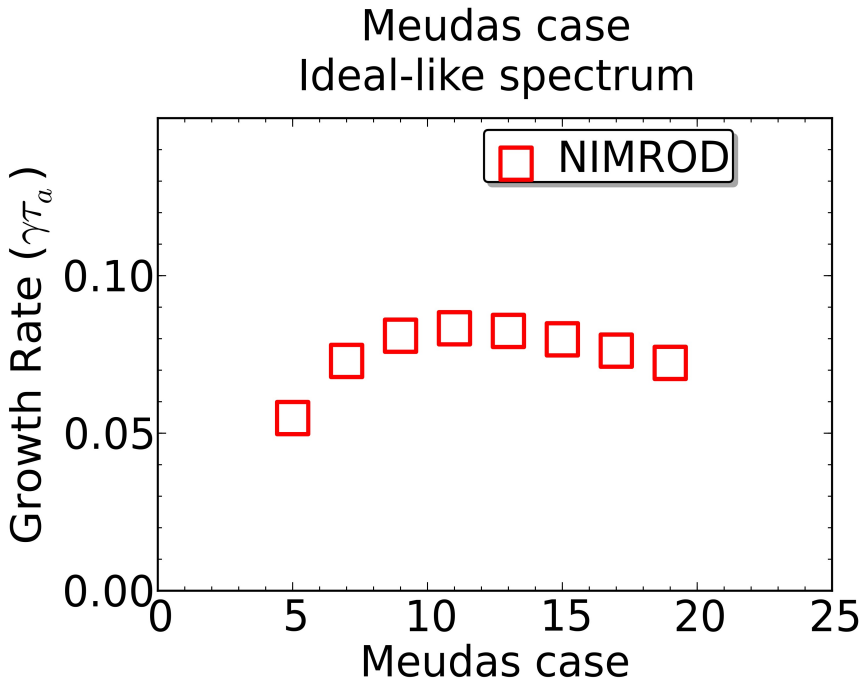

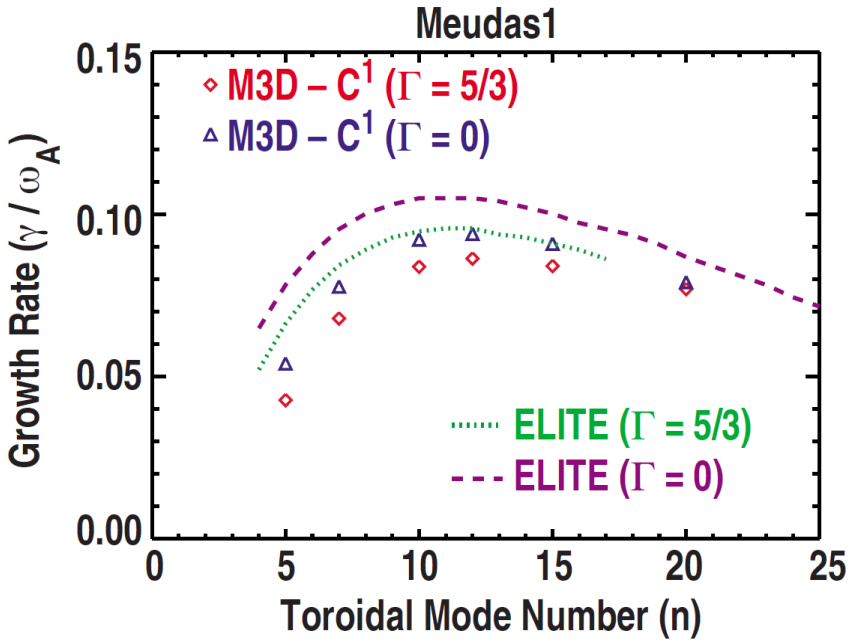

Ferraro et al. (2010)

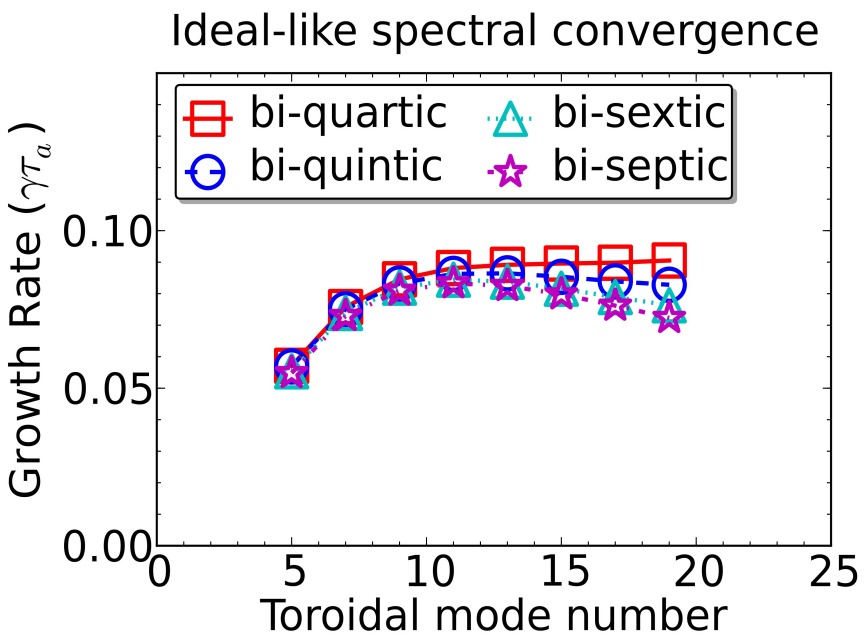

The eigenmode is qualitatively similar to that seen by M3D-C1, although the NIMROD wall location differs.

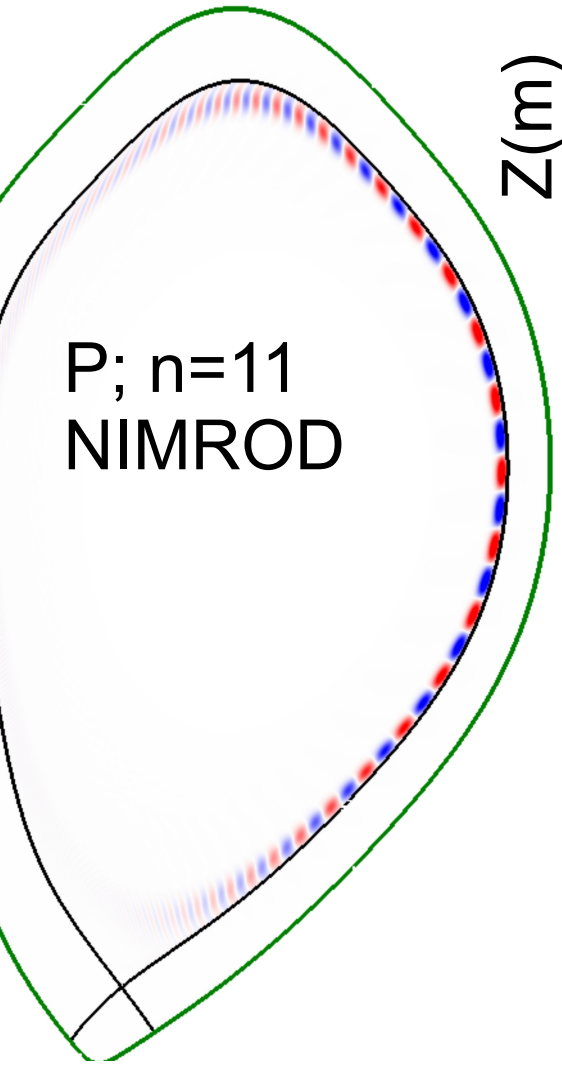

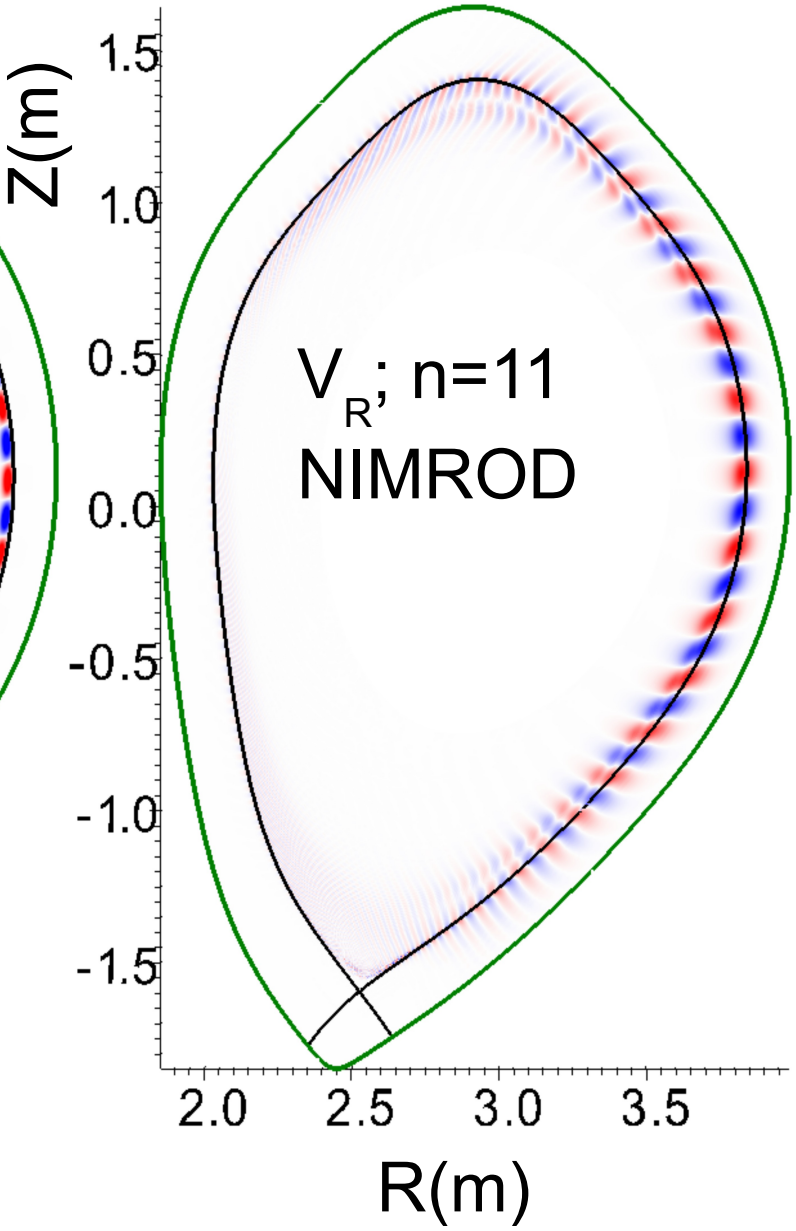

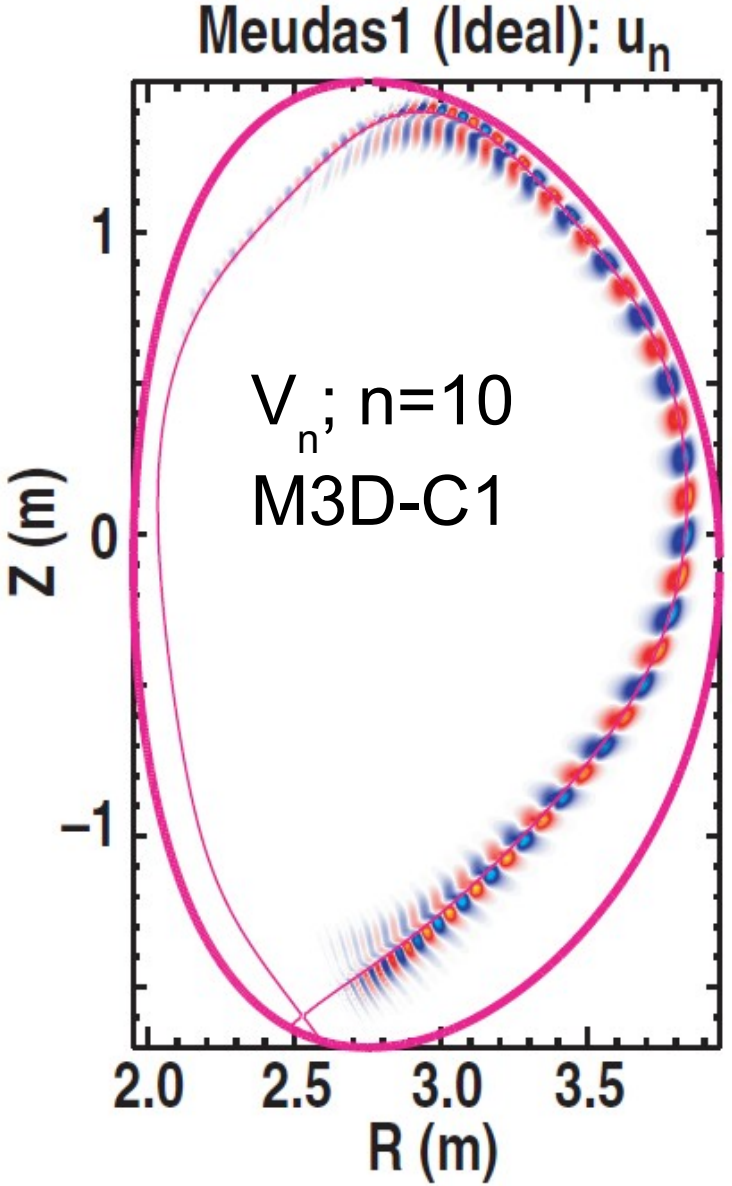

Ferraro et al. (2010)

Convergence depends on resolving in a “diffraction pattern” from interference of inboard and outboard structure near the x-point.

B_R; n=11

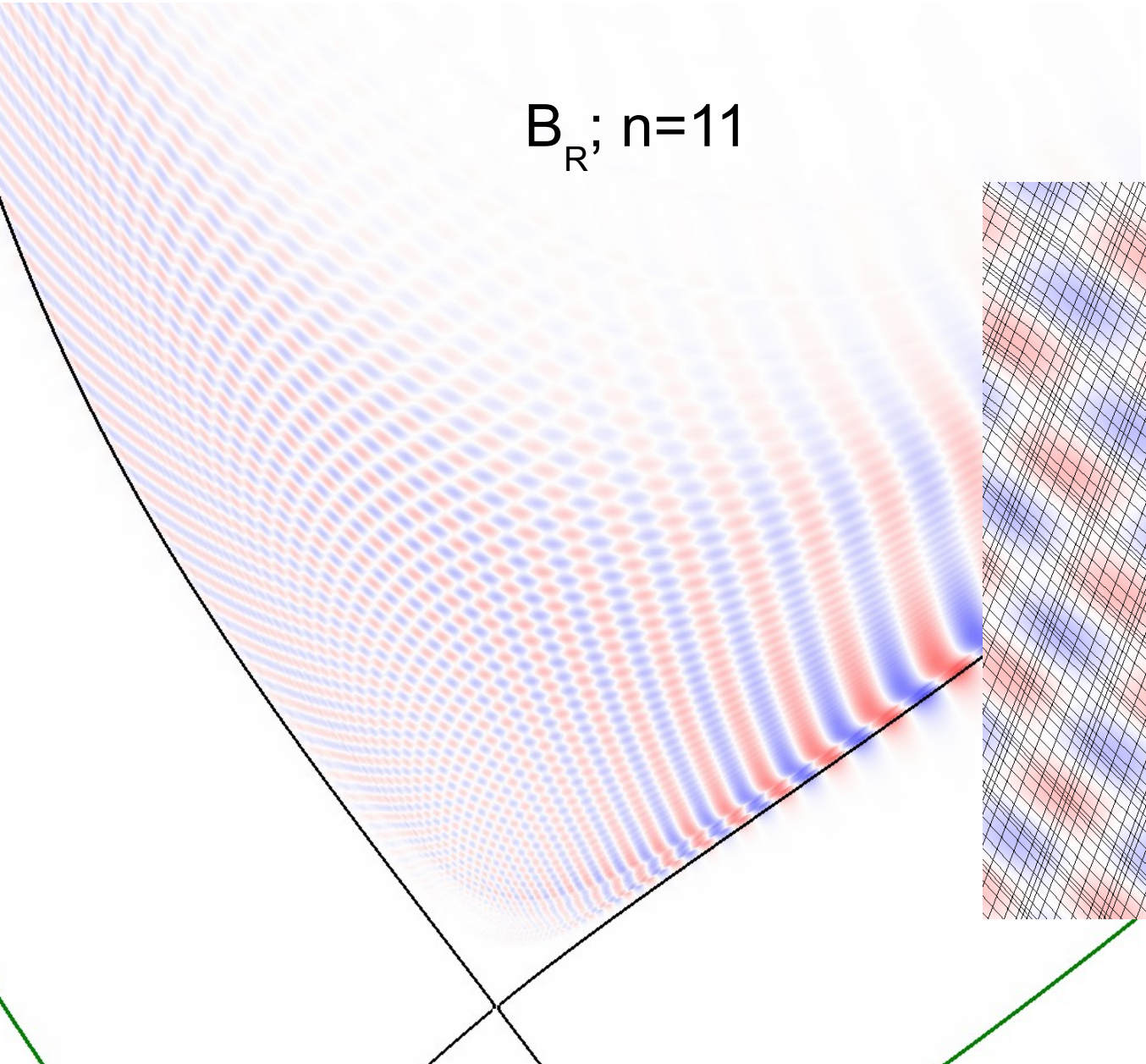

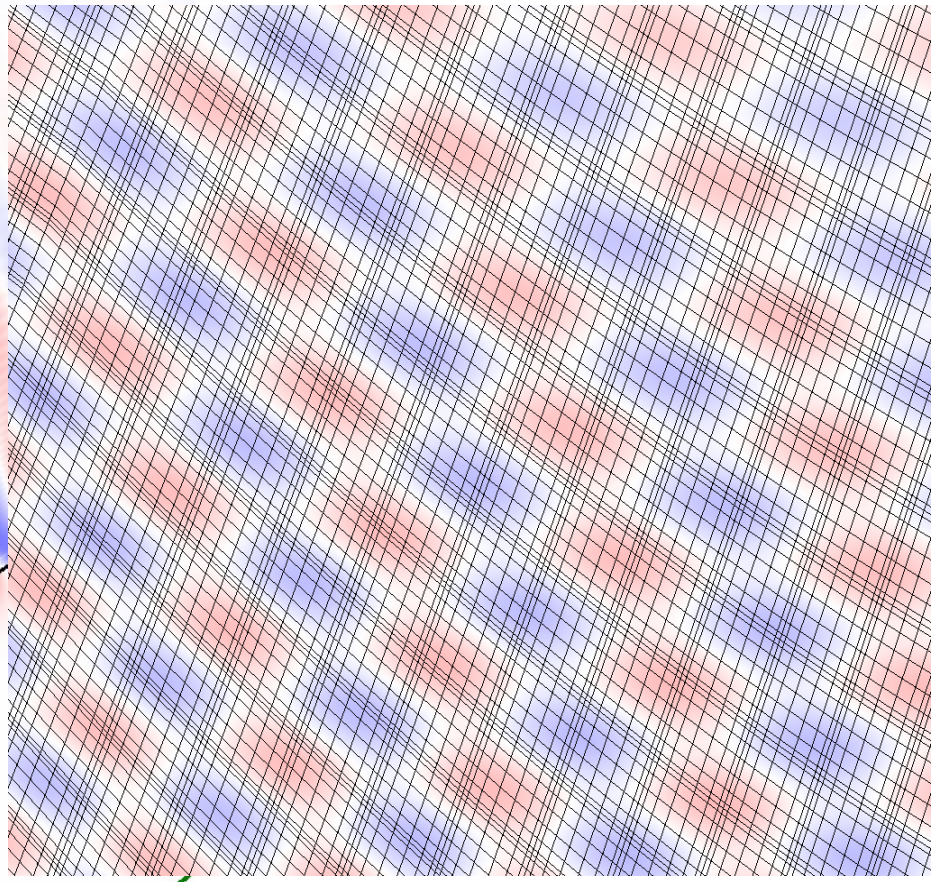

We transition from the ideal-like limit by incrementally adding a density-profile gradient and a temperature-dependent Spitzer resistivity profile.

- We run each model case twice with differing profiles with vacuum temperatures of 50 and 100 eV.
- Visually, the difference between the 50eV and 100eV profiles is small.

Ideal-like profiles

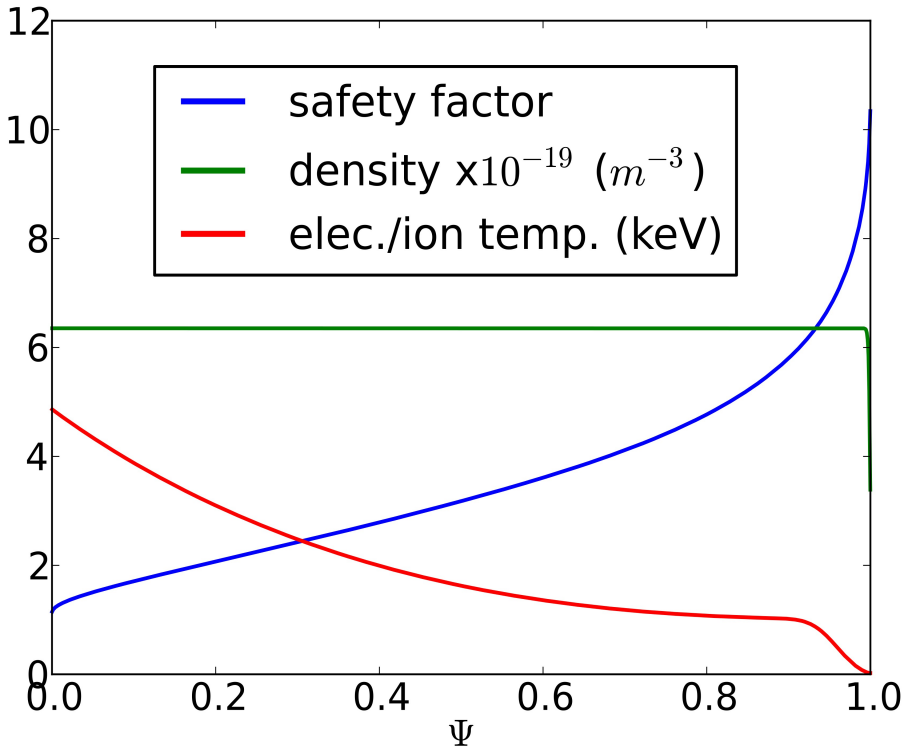

$T_e(\Psi=1) = 100eV$

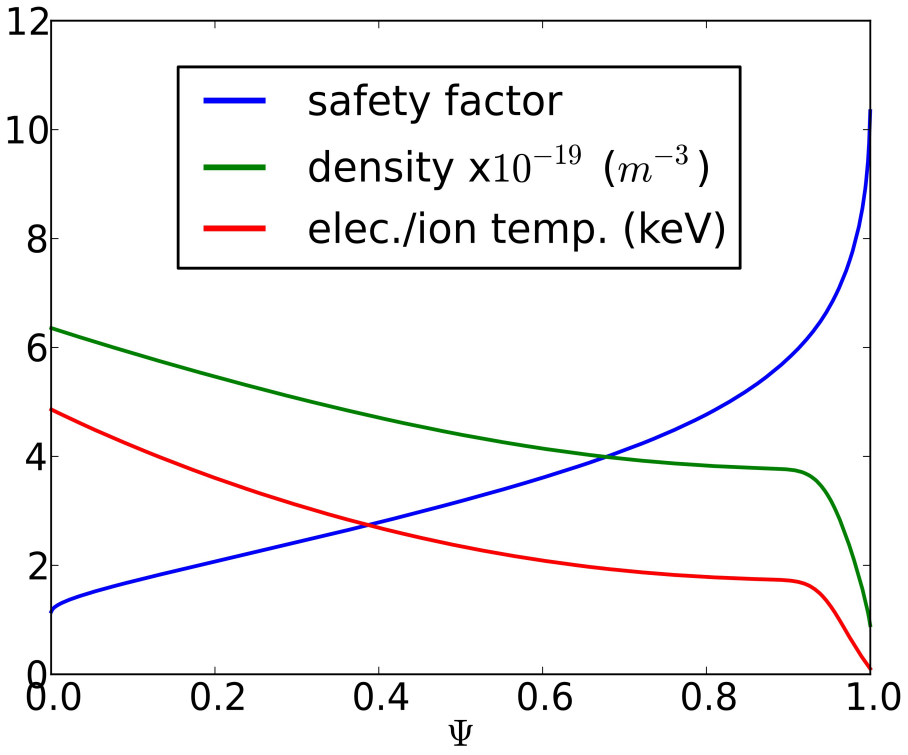

Similar to previous results, the use of a density-profile gradient is destabilizing, however the use of Spitzer-resistivity profiles produces a destabilization of the high-n mode spectrum.

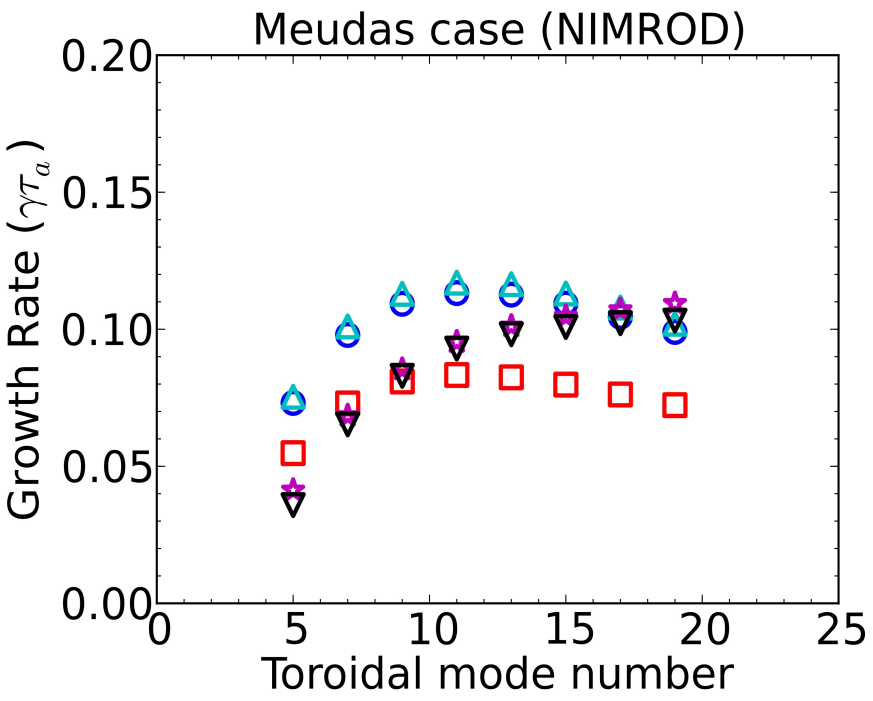

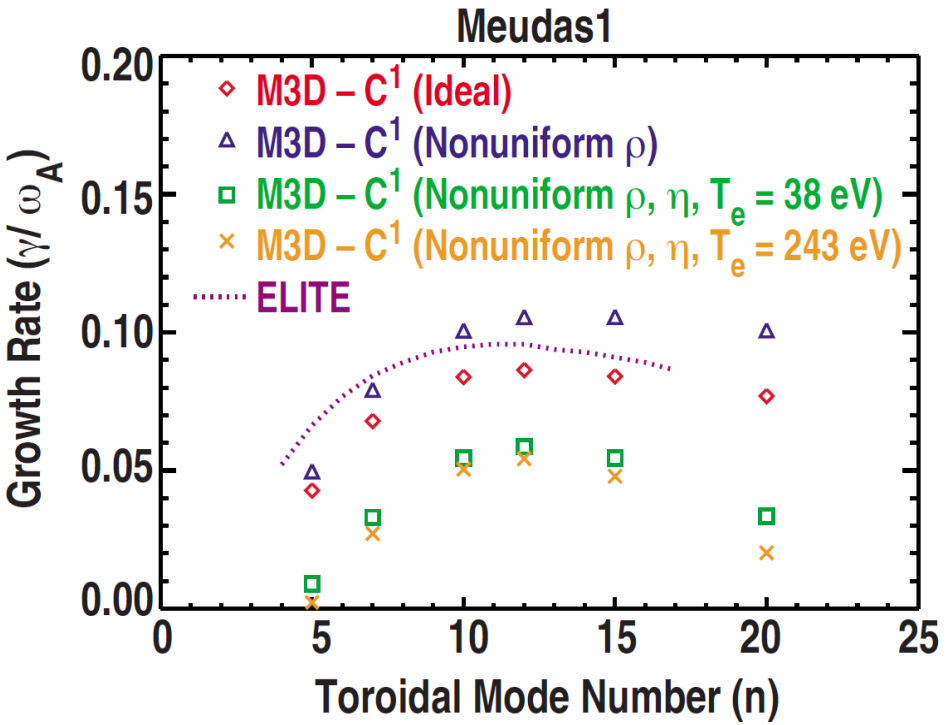

Ferraro et al. (2010) (profiles differ)

- Renormalization of the MHD equations shows ideal frequencies scale as $\rho^{1/2}$.
- With the profiles (which differ with those used by M3D-C1) used in the NIMROD computations, the low-n modes are stabilized and high-n modes are destabilized when a Spitzer-resistivity profile is used.

The extended-MHD model captures parallel-physics, finite-Larmor-radius, and two-fluid effects.

$$\frac{\partial n}{\partial t} + \mathbf{v}\cdot\nabla n = -n\nabla\cdot\mathbf{v} + D_n\nabla^2 n$$

$$m_i n\frac{\partial \mathbf{v}}{\partial t} + m_i n\mathbf{v}\cdot\nabla\mathbf{v} = \mathbf{J}\times\mathbf{B} - \nabla p - \nabla\cdot\mathbf{\Pi} - \nabla\cdot\nu m_i n\mathbf{W}$$

$$\frac{n}{\Gamma-1}\left(\frac{\partial T}{\partial t} + \mathbf{v}\cdot\nabla T\right) = -nT\nabla\cdot\mathbf{v} + \nabla\cdot\left(n\chi_{\parallel}\hat{\mathbf{b}}\hat{\mathbf{b}}\cdot\nabla T\right)$$

$$\mathbf{\Pi} = \frac{m_\alpha p_\alpha}{4eB}\left[\hat{\mathbf{b}}\times\mathbf{W}_\alpha\cdot\left(\mathbf{I}+3\hat{\mathbf{b}}\hat{\mathbf{b}}\right) - \left(\mathbf{I}+3\hat{\mathbf{b}}\hat{\mathbf{b}}\right)\cdot\mathbf{W}_\alpha\times\hat{\mathbf{b}}\right]$$

$$+\nu_{\parallel}m_i n\left(\hat{\mathbf{b}}\hat{\mathbf{b}} - \frac{1}{3}\mathbf{I}\right)\left(3\hat{\mathbf{b}}\cdot\nabla\mathbf{v}_\alpha\cdot\hat{\mathbf{b}} - \nabla\cdot\mathbf{v}_\alpha\right)$$

$$\mathbf{E} = -\mathbf{v}\times\mathbf{B} + \frac{\mathbf{J}\times\mathbf{B}}{ne} - \frac{\nabla p_e}{ne} + \eta\mathbf{J} - \frac{m_e}{e}\frac{\partial \mathbf{v}_e}{\partial t}$$

$$\frac{\partial \mathbf{B}}{\partial t} = -\nabla\times\mathbf{E} \qquad \mu_0\mathbf{J} = \nabla\times\mathbf{B} \qquad p_\alpha = nT_\alpha$$

Before adding extended-MHD effects, the viscosity and perpendicular thermal conductions are enhanced which causes a slight stabilization of the high-n mode spectrum.

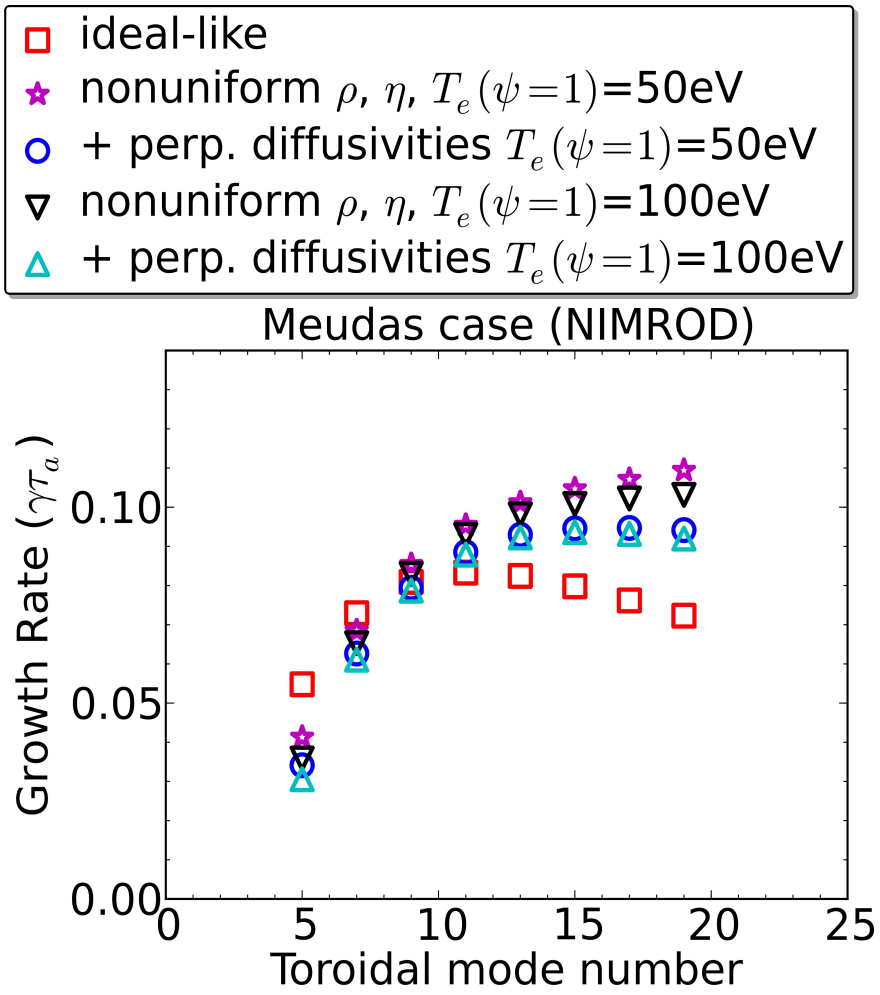

- The NIMROD semi-implicit operator is dispersive, but not dissipative. The ideal-like and other previously shown cases used small explicit dissipation coefficients:

$$P_m = 10^{-3} \qquad \frac{\chi_\perp}{\eta/\mu_0} = 10^{-3}$$

- As we are now interested in adding extended-MHD effects instead of benchmarking, we add a more reasonably small diffusion:

$$P_m = 1 \qquad \chi_\perp = 0.1\ m^2/s$$

- Technically these are isotropic diffusion operators.

Adding anisotropic thermal conduction has a almost no effect on the growth rate.

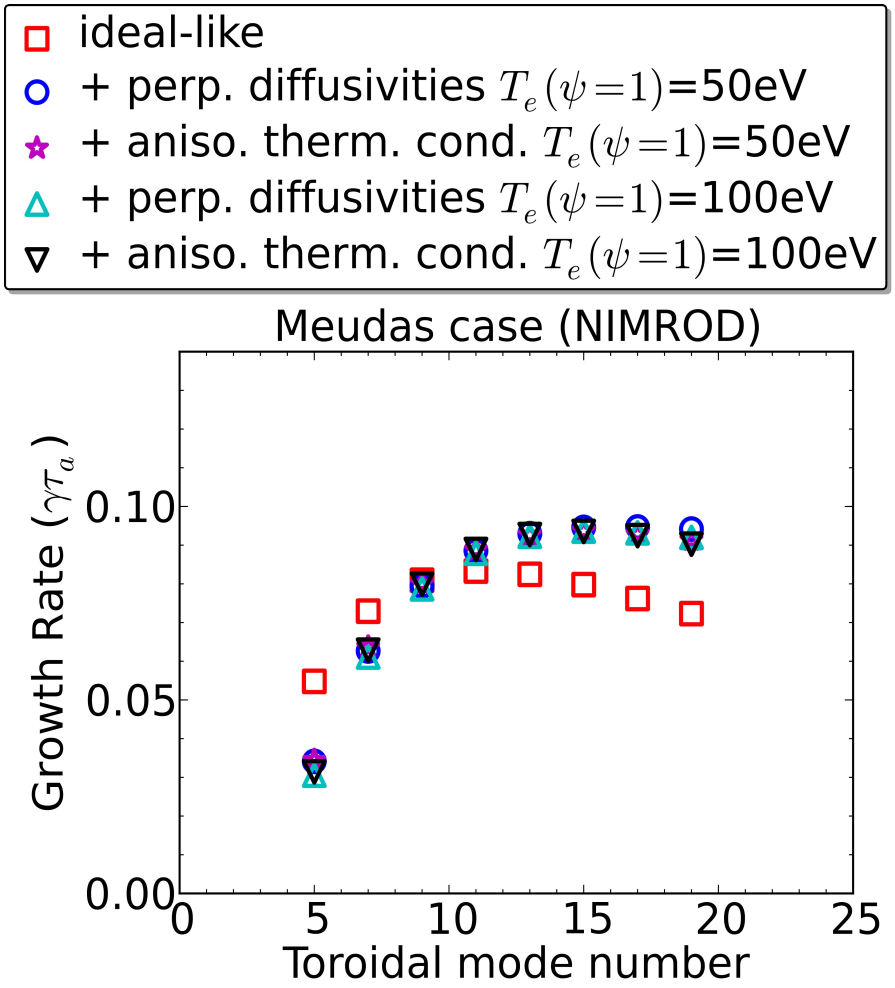

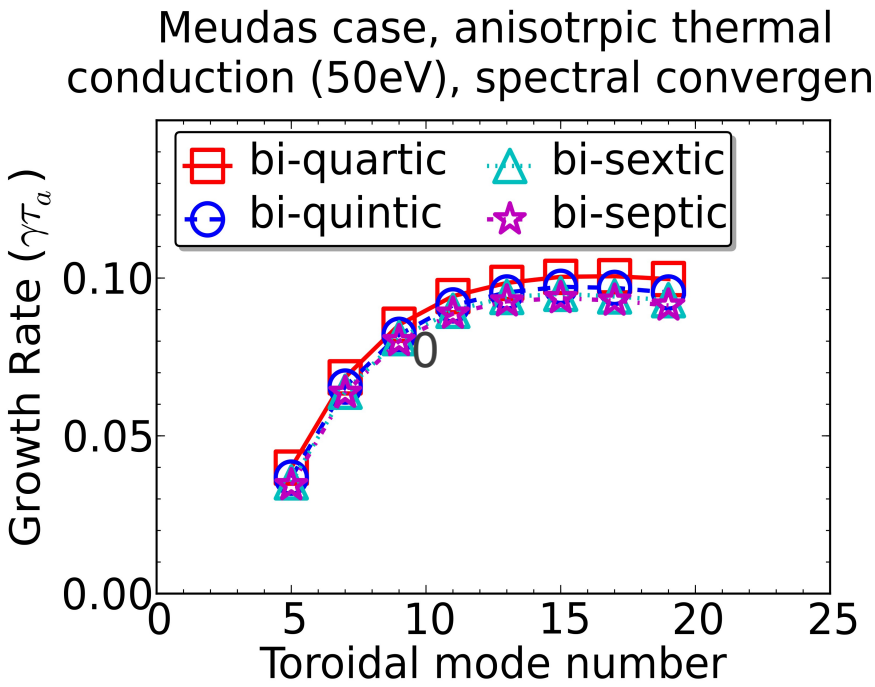

$$\frac{\chi_{\parallel}}{\chi_{\perp}} = 5 \times 10^{8}$$

We expect the importance of the two-fluid and drift effects to be enhanced at higher temperature.

Mag. Axis, 4845eV	Mag. Sep., 100eV	Mag. Sep., 50eV
$\beta = 0.01$	$\beta = 3.2 \times 10^{-5}$	$\beta = 1.7 \times 10^{-5}$
$d_i = 0.02\ m$	$d_i = 0.05\ m$	$d_i = 0.05\ m$
$\rho_i = 0.002\ m$	$\rho_i = 0.0003\ m$	$\rho_i = 0.0002\ m$

- Our model is first order in ion gyroradius, and thus is formally valid only up to intermediate-wavenumber edge-resonant modes.
- However, the model may be qualitatively descriptive for large wavenumbers.
- The parameters and modes studied for this case are reasonably within the range of model validity.

$$k_{n6}\rho_i = 0.0018$$
$$k_{n15}\rho_i = 0.0045$$
$$k_{n43}\rho_i = 0.013$$

$$\begin{aligned} k &\simeq n/R + m/r_s \\ &\simeq n/R + nq(r_s)/r_s \\ &\simeq 10n \end{aligned}$$

Ion gyroviscosity is stabilizing to the high-n mode spectrum and this stabilization is enhanced at higher temperatures.

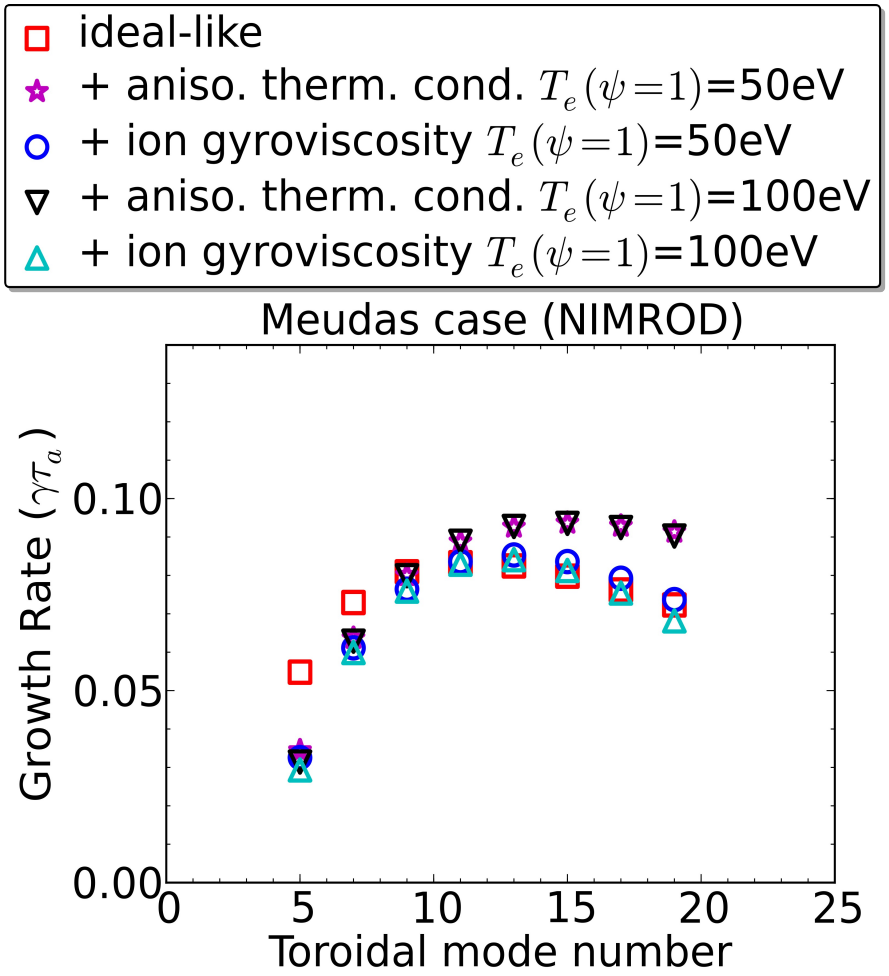

- BOUT++ results compare a gyro-fluid model with a reduced extended-MHD model and find that agreement between the models (and stabilization of this high-n spectrum) requires ion gyroviscosity, and, in particular, a full ion gyroviscosity with corrections beyond the "gyroviscous cancellation" [2].

[2] Xu et al., APS invited talk (2012)
https://bout.llnl.gov/pdf/meetingPresentations/APS/2012/TI3xu.pdf

The growth rate becomes complex (mode rotation) when ion gyroviscosity is present in the model.

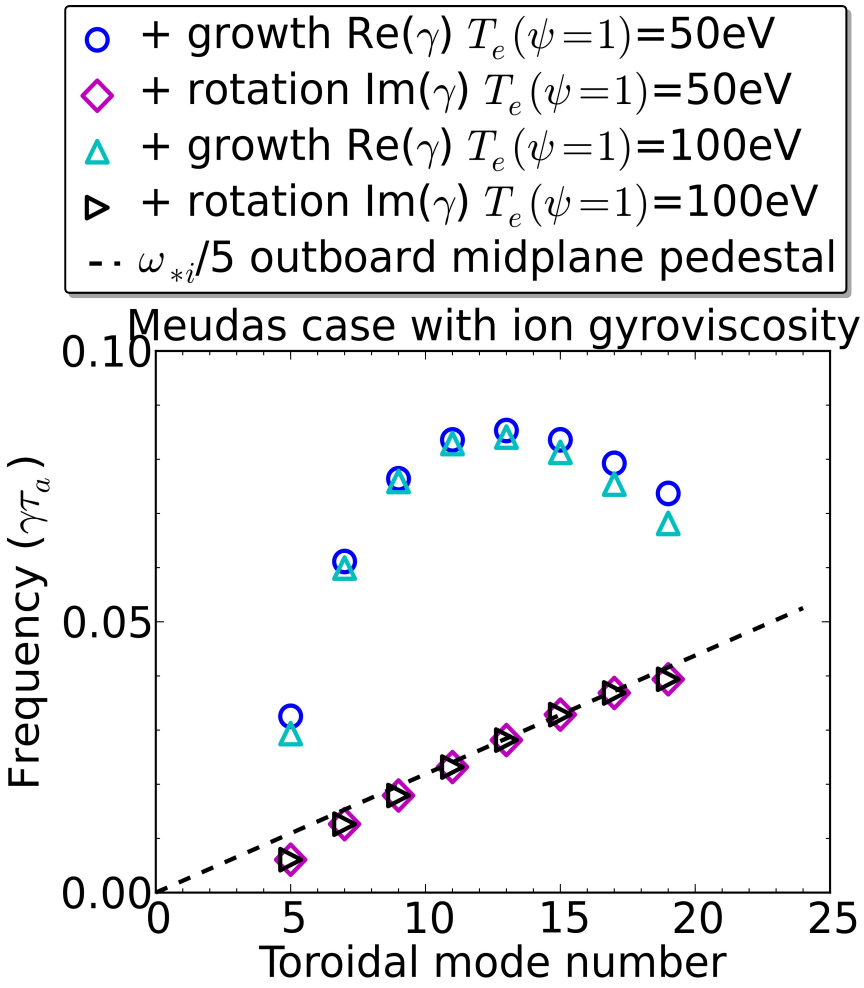

- This case has no equilibrium flow; the ExB flow is assumed to cancel the diamagnetic flow.
- The use of ion gyroviscosity introduces drifts proportional to the diamagnetic frequency (diamagnetic cancellation), as well as drifts proportional to the gradient of B and magnetic curvature [3], however, these latter drifts are relatively small in the pedestal.

[3] King, Sovinec and Mirnov Phys. Plasmas 18, 042303 (2011)

Before using a generalized Ohm's law, we add a small amount of density diffusivity which produces a minimal impact on the growth rate.

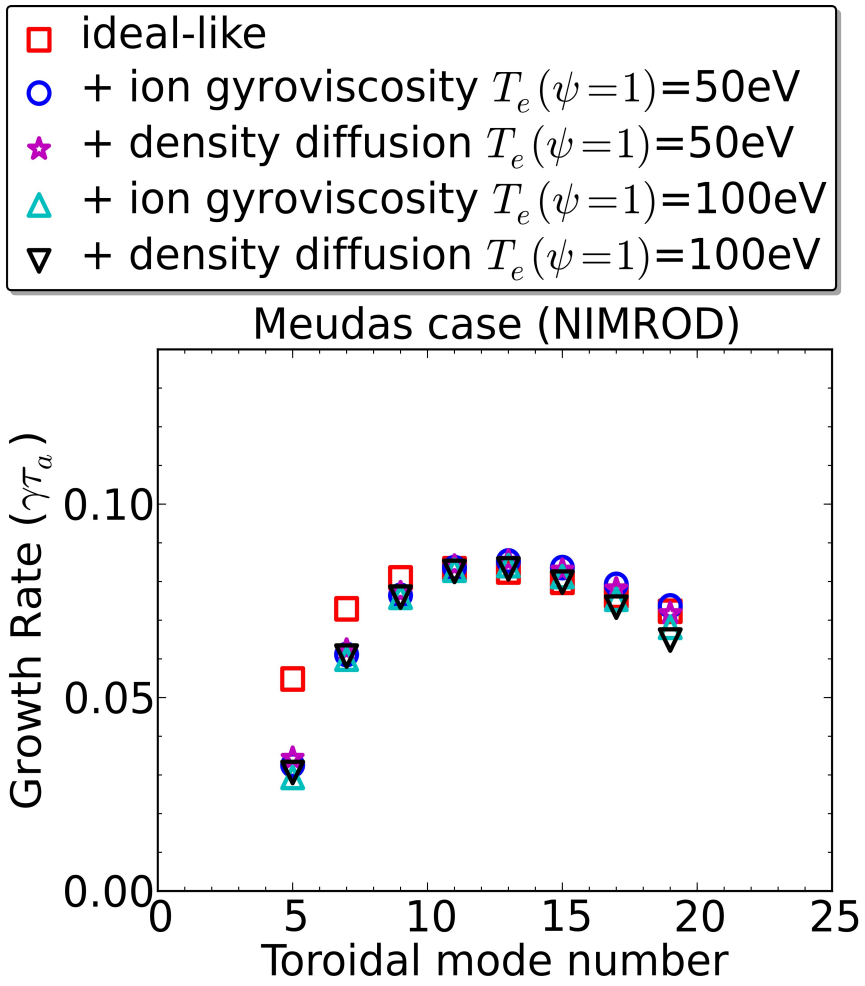

- This is necessary for numerical stability when the generalized Ohm's law is used.
- In this case, the density perturbation is coupled to magnetic field update by the gradient of the electron pressure term.
- We also use a small amount of density hyper-diffusivity.

$$D_n = 0.1\ m^2/s$$

$$\frac{D_{n,hyper}/a^2}{\eta/\mu_0} = 5 \times 10^{-4}$$

With the use of a generalized Ohm's law, the growth rate is enhanced at intermediate n, and stabilized at high n.

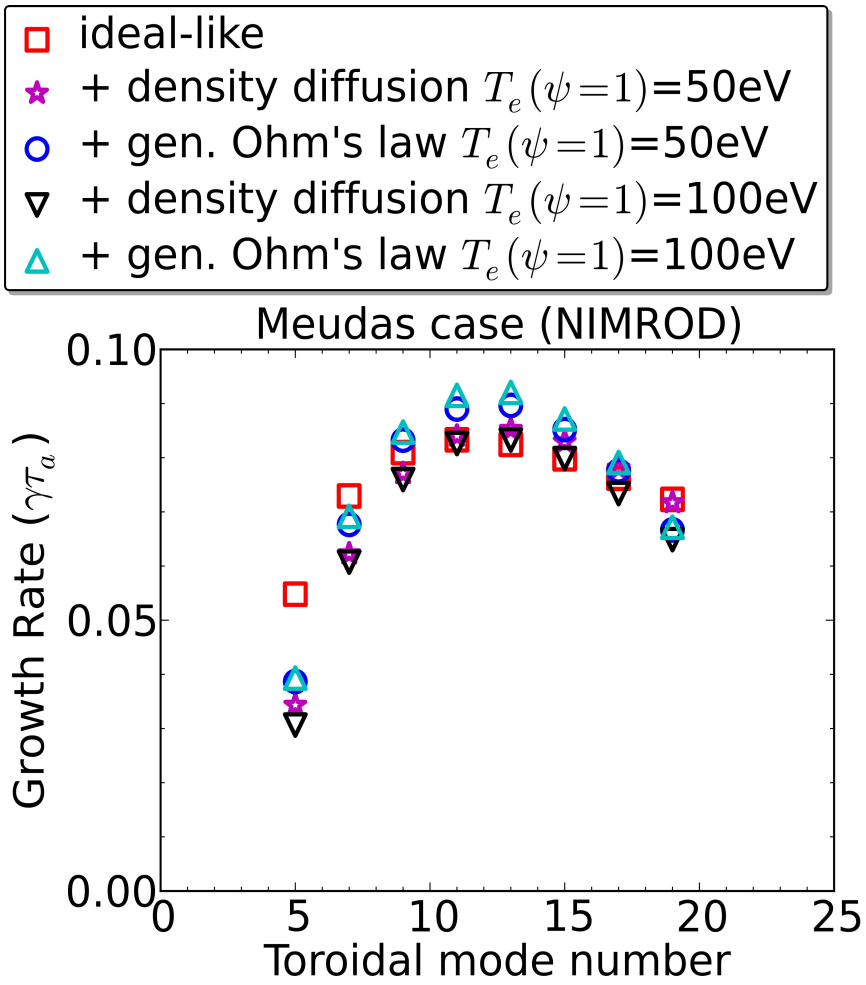

- The use of the generalized Ohm's law introduces ion-electron fluid decoupling and additional drift effects into the model.
- The growth rate enhancement for intermediate-n modes and stabilization for high-n modes is qualitatively similar to that theoretically predicted in Ref. [4].

[4] Hastie, Ramos and Porcelli Phys. Plasmas 10, 4405 (2003)

The inclusion of ion parallel viscosity does not significantly modify the growth-rate spectrum.

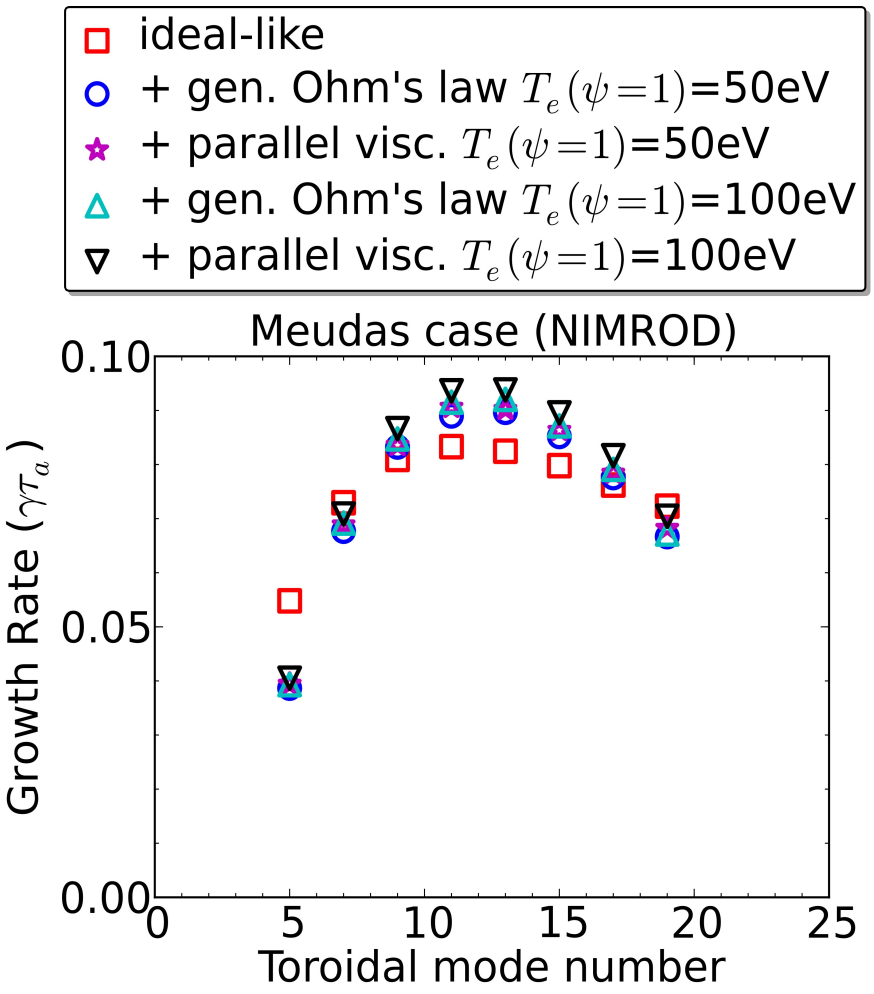

- The coefficient of the ion parallel viscosity term is based on the separatrix temperature.

$$T_e = 100eV: \quad \nu_{||} = 5 \times 10^4\ m^2/s$$

$$T_e = 50eV: \quad \nu_{||} = 9 \times 10^3\ m^2/s$$

- There is a slight increase in the growth rate of the Te=100eV cases, and a larger coefficient, as would be expected in higher temperature regions may have a more significant impact.

There are still additional effects from terms in the extended-MHD model that remain unexplored.

- As the bootstrap current is significant in these edge cases, it is of interest to implement and study the effect of electron parallel viscosity.
- The implementation of electron parallel viscosity would add an auxiliary variable to the magnetic field advance [5], which makes the recent memory enhancements all the more important.
- It is also of interest to use separate energy equations for the electrons and ions such that drift effects from diamagnetic heat flows are properly modeled.
- However, separate energy equations are numerically challenging as one must model the fast advection of parallel electron flows in the electron energy equation.
- Additionally, ion temperature gradient modes may be unstable and are, at least partially, captured by the extended-MHD model [6].

[5] Sovinec, “A Formulation of Fluid Parallel Electron Viscosity for NIMROD” from http://www.cptc.wisc.edu/sovinec_research

[6] Schnack et al., “Local ITG-like Instability in the Two-fluid and Extended MHD Models in Slab Geometry” UW-CPTC 12-2 from http://www.cptc.wisc.edu

Summary

- We have made improvements to the NIMROD code that have enabled previously unachievable simulations.
- With these improvements, we have successfully benchmarked the diverted, high-q_{95} 'meudas' case with ELITE.
- The transition from an ideal-like to an extended-MHD model has been investigated for this case:
  - Similar to BOUT++ results [2 (Xu et al.)], ion gyroviscosity is found to be stabilizing to the high-n growth-rate spectrum.
  - The low-n spectrum is destabilized and the high-n spectrum stabilized by the use of a generalized Ohm's law, which is in qualitative agreement with analytic theory [4 (Hastie, Ramos and Porcelli)].
  - Large parallel conductivity and ion parallel viscosity do not have a significant effect on the growth-rate spectrum.
- Realistic density and resistivity profiles destabilize and two-fluid, FLR effects stabilize the high-n growth-rate spectrum relative to ideal MHD.
- Using the enhancements to the memory management in NIMROD, we can now return to relatively high-q_{95} cases with edge harmonic oscillations (EHO).

Convergence of the growth-rate spectrum with the extended-MHD model.

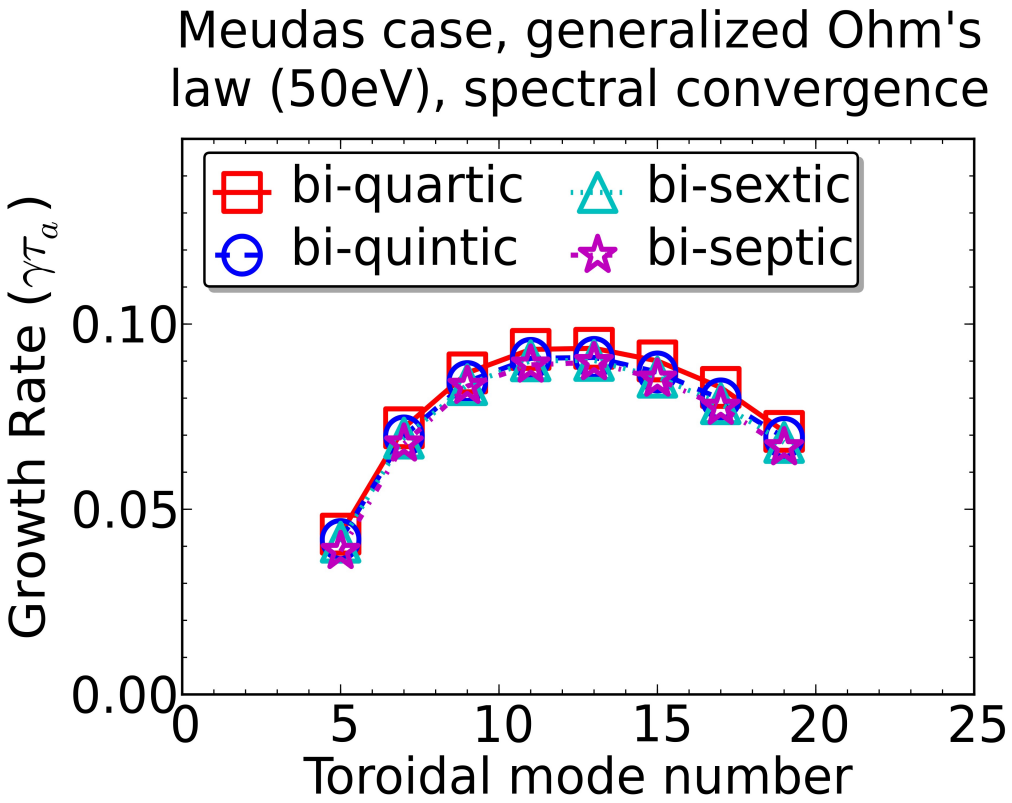

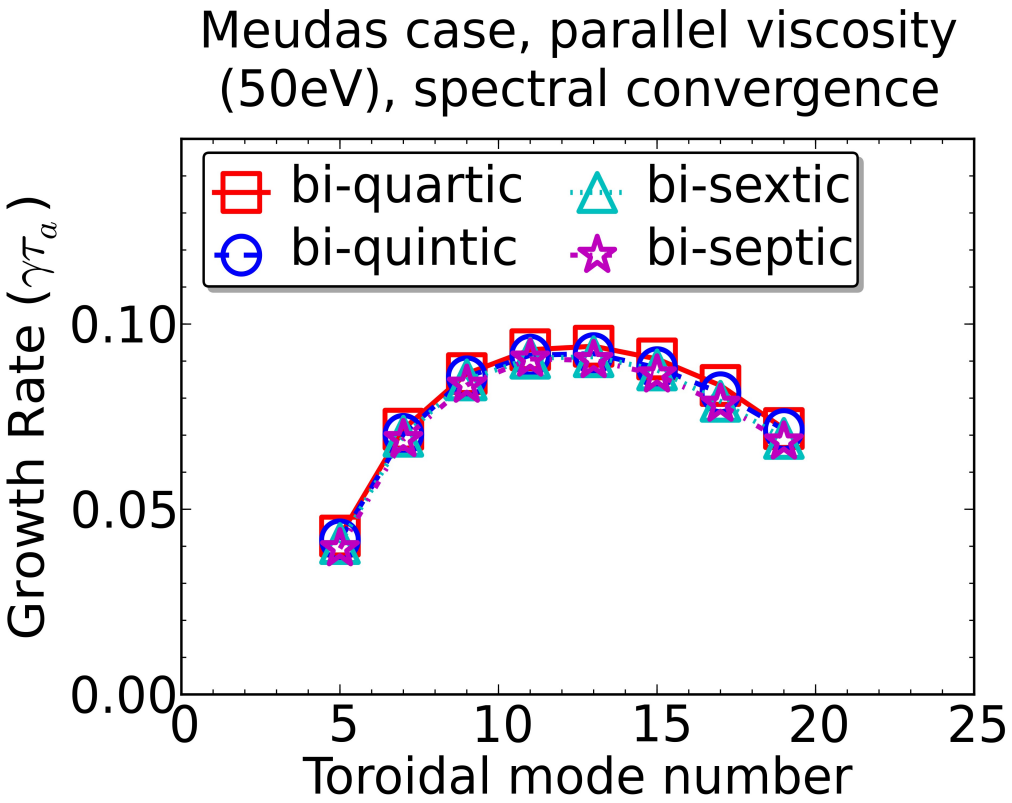

The macroscopic structure of the eigenfunction does not change significantly with different models.